Published in final edited form as:

Connect Tissue Res. 2014 August ; 55(0 1): 134–137. doi:10.3109/03008207.2014.923870.

The role of phosphorylation in dentin phosphoprotein peptide absorption to hydroxyapatite surfaces: a molecular dynamics study

Eduardo Villarreal-Ramirez[1,2,3], **Ramon Garduño-Juarez**[2], **Arne Gericke**[3], and **Adele Boskey**[1]

[1]Mineralized Tissue Research Laboratory, Hospital for Special Surgery, New York, NY, USA

[2]Departmento de biofísica, Instituto de Ciencias Físicas, UNAM, Cuernavaca, México

[3]Department of Chemistry and Biochemistry, Worcester Polytechnic Institute, Worcester, MA, USA

Abstract

Dentin phosphoprotein (DPP) is a protein expressed mainly in dentin and to a lesser extent in bone. DPP has a disordered structure, rich in glutamic acid, aspartic acid and phosphorylated serine/threonine residues. It has a high capacity for binding to calcium ions and to hydroxyapatite (HA) crystal surfaces. We used molecular dynamics (MD) simulations as a method for virtually screening interactions between DPP motifs and HA. The goal was to determine which motifs are absorbed to HA surfaces. For these simulations, we considered five peptides from the human DPP sequence. All-atom MD simulations were performed using GROMACS, the peptides were oriented parallel to the {100} HA crystal surface, the distance between the HA and the peptide was 3 nm. The system was simulated for 20 ns. Preliminary results show that for the unphosphorylated peptides, the acidic amino acids present an electrostatic attraction where their side chains are oriented towards HA. This attraction, however, is slow to facilitate bulk transport to the crystal surface. On the other hand, the phosphorylated (PP) peptides are rapidly absorbed on the surface of the HA with their centers of mass closer to the HA surface. More importantly, the root mean square fluctuation (RMSF) indicates that the average structures of the phosphorylated peptides are very inflexible and elongate, while that of the unphosphorylated peptides are flexible. Radius of gyration (Rg) analysis showed the compactness of un-phosphorylated peptides is lower than phosphorylated peptides. Phosphorylation of the DPP peptides is necessary for binding to HA surfaces.

Keywords

Biomineralization; bone dentin; dentin phosphoprotein; molecular dynamics; phosphophoryn

Correspondence: Dr Adele Boskey, Hospital for Special Surgery, Mineralized Tissue Laboratory, Caspary Research Building 541 East 71st Street 6 Floor, New York, NY 10021, USA. boskeya@hss.edu.

Declaration of interest

The authors declare no conflict of interest.

Introduction

The mechanism of deposition of physiologic hydroxyapatite (HA) crystals in collagen-based tissues (bone, dentin, cementum, calcified cartilage, etc.) is a poorly understood complex process (1). It is generally accepted that during HA formation both collagen and noncollagenous proteins (NCPs) regulate the nucleation, growth and inhibition of HA (2). Dentin phosphoprotein (DPP) is expressed mainly in dentin and to a lesser extent in bone. DPP is the most acidic protein ever discovered in mammals (pI 1.1) (3). It is particularly rich in aspartic acid and serine, with up to 90% of all serines phosphorylated. DPP is the most abundant phosphoprotein (PP) in dentin and plays a critical role in its mineralization. DPP has been implicated in the mineralization process of bone and dentin by its ability to regulate both initial mineralization and remodeling. DPP shows a high capacity for binding to calcium ions (Ca^{2+}) and HA crystal surfaces (4-6).

Computer modeling and molecular dynamics (MD) simulations are a fast and relatively inexpensive option to screen specific molecular recognition between interacting molecules. Several studies have used MD simulations to show that proteins are generally adsorbed by electrostatic forces of different strengths, depending on the protein's structure and surface charge (7-10). However, key interactions between DPP and HA are not known. The goal of this study is to determine which DPP motifs are absorbed to HA surfaces. We studied the HA binding domains of DPP by using a peptide screening model and applying MD simulation to elucidate the key interactions between DPP and HA. We also analyzed the role of phosphorylation in the flexibility of DPP-peptides in solution and when absorbed to HA.

Methods

GROMACS version 4.5.3 (11) was used to perform MD. Five different peptides extracted from the highly recurrent sequences of DPP were investigated (Table 1). These peptides, cover to a large extent, the complete motifs observed in DPP (12). The peptides were modeled in their extended conformations and capped at their sequence termini (PyMol and YASARA). The peptides were phosphorylated according to the predictions performed by the NetPhos 2.0 server. Steepest descent minimization was performed on all peptide models before performing MD. HA mineral has a hexagonal structure with space group $P6_{3/m}$. The unit cell parameters are a = 9.424 Å °, b = 9.424 Å °, c = 6.853 Å °, alpha = 90°, beta = 90°, gamma = 120° (7). The HA supercell was modeled according to Mostafa et al. (13). We used the GULP program to optimize the geometry of the HA supercell.

This communication presents results from MD simulations with GROMACS version 4.5.3 and the GROMOS96 43a1p force field supplemented with HA parameters (14). The simulations were performed in the NVT ensemble at 300° K and periodic boundary conditions were applied in rectangular boxes with 5.6 nm × 6.8 nm in the plane of the surface and 9 nm perpendicular to the surface. In our MD simulations, we used the SHAKE algorithm to constrain the bond lengths. For the Lennard–Jones interactions, we used a 1.0 nm cutoff. For all simulations we used simple point charge (SPC) water. The peptides in solution were positioned at the center of the box, whereas the peptides with HA were oriented parallel to the {100} crystal face where the distance between the HA slab and the

peptide was 3 nm. Prior to the actual simulation, energy minimization was performed without constraints using the steepest descent method. All systems were simulated for 20 ns.

Results

Preliminary results show that all DPP-derived peptide sequences were attracted to the HA surface, mainly by electrostatic interactions between the negatively charged peptides residues and the positive charges in HA. This attraction is strong enough to facilitate bulk transport from the peptide in solution to the crystal surface. Furthermore, the phosphorylated peptides (PP) had a greater affinity, resulting in a stronger attraction to HA surface and in a shorter time than their unphosphorylated counterparts. Some unphosphorylated peptides needed more than 10 ns to be fully absorbed to the HA surface (Supplementary Figure 1). The unphosphorylated peptides show a lower compactness based on their radius of gyration (Rg) relative to the phosphorylated peptides. That means that the unphosphorylated peptides can fold over the HA surface, whereas the phosphorylated peptides are linear over the HA surface (Figure 1). Interestingly, the unphosphorylated peptides displayed higher mobility than the phosphorylated peptides, as indicated from the calculation of the root mean square fluctuation (RMSF) illustrated for peptide 1 (Figure 2). To determine whether this behavior is due to the phosphorylation or to the absorption to HA surfaces, we carried out MD simulations of each of the peptides in an HA-free state. We observed that the most rigid peptides were the phosphorylated peptides bound to HA, while the most flexible peptides were the unphosphorylated peptides in an HA-free state. Peptide 5 had a distinct behavior; unphosphorylated peptide 5 was less flexible than its phosphorylated partner (data not shown). The B-factors analyses showed that each peptide's dynamics differed between phosphorylated and unphosphorylated forms. The average structure of peptide 1 and 1P was independent of adsorption state, whereas the average structure of peptide 2-HA and 2P-HA displayed some similarities (Figure 1, Supplementary Figure 2).

Discussion

DPP has an important role in biomineralization of dentin; mutations in this protein cause dentinogenesis imperfecta. DPP is specifically located at the mineralization front suggesting that it regulates the mineralization process (15). According to our MD results, the net charge of the DPP peptides has great consequence with respect to their average structure and their binding affinity to HA surfaces. The phosphorylated peptides with the greatest negative charge can bind to HA surfaces with greater affinity than unphosphorylated peptides. The specific role of lysines in peptide 2 is still unclear, but due to their positive charge, these amino acids were distant from HA (Supplementary Figure 2). These results are consistent with those of other studies (7) showing that phosphorylated peptides also can bind to the HA surface more rapidly than unphosphorylated peptides. Of note, the average structure of the peptides and the dynamics of the peptides are closely related to their total charge, while conformation changes for binding partners are unclear. The phosphorylation pattern is relevant to the average structure of the peptides even if they are in solution. However, experimental studies of peptides have shown that phosphorylation stabilizes α-helix formation (16). Therefore, the DPP phosphorylation pattern could be a code for the configurations of the peptides and hence their affinity for potential ligands. In previous

studies, we showed the important role of phosphorylation in mineralized tissues and its role in the biomineralization process (17,18); this study showed the specific behavior of the DPP peptides when they are phosphorylated. The precise role of each of the peptide structures remains unclear. However, as MD is sensitive to initial conditions, we will compare these preliminary MD data with experimental in vitro results to refine the initial conditions before applying others sophisticated computational techniques (9).

Conclusion

We successfully screened HA binding motifs of human DPP sequences; peptides 1 and 5 were the sequences with greatest predicted affinity for HA. We will confirm these results by more robust MD protocols such as umbrella sampling and biophysical techniques to confirm these preliminary findings. The preliminary data indicate that the diverse function of DPP and perhaps other acidic matrix proteins in different tissues is highly dependent on their degree of phosphorylation.

Supplementary Material

Refer to Web version on PubMed Central for supplementary material.

Acknowledgments

We thank Ulises Amaya Olvera (Instituto de Ciencias Físicas at UNAM), Siamak M. Najafi and Raffaele Potami (Research Computing and Academic center at WPI) for technical support. EVR acknowledges financial support received from DGAPA and CONACYT.

Supported by PAPIIT-UNAM IN221913 and the National Institutes of Health (DEO4141-DEO22716).

References

1. Boskey AL. Noncollagenous matrix proteins and their role in mineralization. Bone Mineral. 1989; 6:111–23. [PubMed: 2670018]
2. Boskey AL, Maresca M, Ullrich W, Doty SB, Butler WT, Prince CW. Osteopontin-hydroxyapatite interactions in vitro: inhibition of hydroxyapatite formation and growth in a gelatin-gel. Bone Mineral. 1993; 22:147–59. [PubMed: 8251766]
3. Nanci A. Ten Cate's oral histology – pageburst on vitalsource: development, structure, and function. Elsevier Health Sciences. 2007 Sep 26.:432.
4. Lee SL, Veis A, Glonek T. Dentin phosphoprotein: an extracellular calcium-binding protein. Biochemistry. 1977; 16:2971–9. [PubMed: 406911]
5. Fujisawa R, Kuboki Y. Preferential adsorption of dentin and bone acidic proteins on the (100) face of hydroxyapatite crystals. Biochim Biophys Acta. 1991; 1075:56–60. [PubMed: 1654109]
6. Boskey AL, Maresca M, Doty S, Sabsay B, Veis A. Concentration-dependent effects of dentin phosphophoryn in the regulation of in vitro hydroxyapatite formation and growth. Bone Mineral. 1990; 11:55–65. [PubMed: 2176557]
7. Pan HH, Tao JH, Xu XR, Tang RK. Adsorption processes of Gly and Glu amino acids on hydroxyapatite surfaces at the atomic level. Langmuir: ACS J Surface Colloid. 2007; 23:8972–81.
8. Azzopardi PV, O'Young J, Lajoie G, Karttunen M, Goldberg HA, Hunter GK. Roles of electrostatics and conformation in protein-crystal interactions. PLoS ONE. 2010; 5
9. Xu ZJ, Yang Y, Wang ZQ, Mkhonto D, Shang C, Liu ZP, et al. Small molecule-mediated control of hydroxyapatite growth: free energy calculations benchmarked to density functional theory. J Comput Chem. 2014; 35:70–81. [PubMed: 24272540]

10. Bhowmik R, Katti KS, Katti D. Molecular dynamics simulation of hydroxyapatite–polyacrylic acid interfaces. Polymer. 2007; 48:664–74.
11. Van Der Spoel D, Lindahl E, Hess B, Groenhof G, Mark AE, Berendsen HJC. GROMACS: fast, flexible, and free. J Comput Chem. 2005; 26:1701–18. [PubMed: 16211538]
12. McKnight DA, Fisher LW. Molecular evolution of dentin phospho-protein among toothed and toothless animals. BMC Evol Biol. 2009; 9
13. Mostafa NY, Brown PW. Computer simulation of stoichiometric hydroxyapatite: structure and substitutions. J Phys Chem Solid. 2007; 68:431–7.
14. Hauptmann S, Dufner H, Brickmann J, Kast SM, Berry RS. Potential energy function for apatites. Phys Chem Chem Phys. 2003; 5:635–9.
15. George A, Veis A. Phosphorylated proteins and control over apatite nucleation, crystal growth, and inhibition. Chem Rev. 2008; 108:4670–93. [PubMed: 18831570]
16. Smart JL, Mccammon JA. Phosphorylation stabilizes the N-termini of α-helices. Biopolymers. 1999; 49:225–33. [PubMed: 9990840]
17. Boskey AL, Doty SB, Kudryashov V, Mayer-Kuckuk P, Roy R, Binderman I. Modulation of extracellular matrix protein phosphorylation alters mineralization in differentiating chick limb-bud mesenchymal cell micromass cultures. Bone. 2008; 42:1061–71. [PubMed: 18396125]
18. Gericke A, Qin C, Spevak L, Fujimoto Y, Butler WT, Sørensen ES, et al. Importance of phosphorylation for osteopontin regulation of biomineralization. Calci Tissue Int. 2005; 77:45–54.

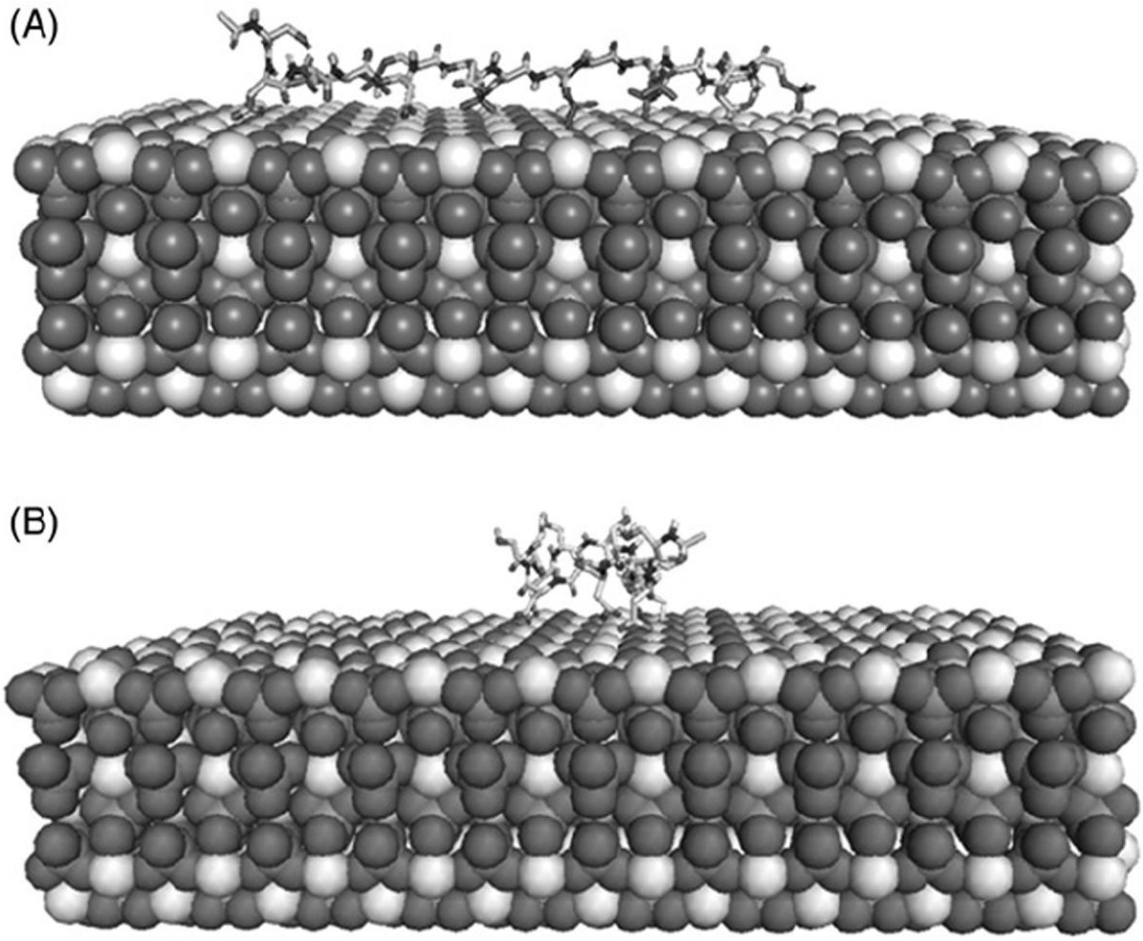

Figure 1.
Molecular-dynamics analysis of Ace-SDSpSDpSDpSpSDp SpSDpSD-NH2 (A) and Ace-SDSSDSDSSDSSDSD-NH2 (B) peptides absorbed to HA. The phosphorylated peptides maintain a linear-like structure and more rigid when they were absorbed to HA, whereas the unphosphorylated peptides were more flexible under the same conditions. The phosphorylated peptides were also absorbed more rapidly to HA.

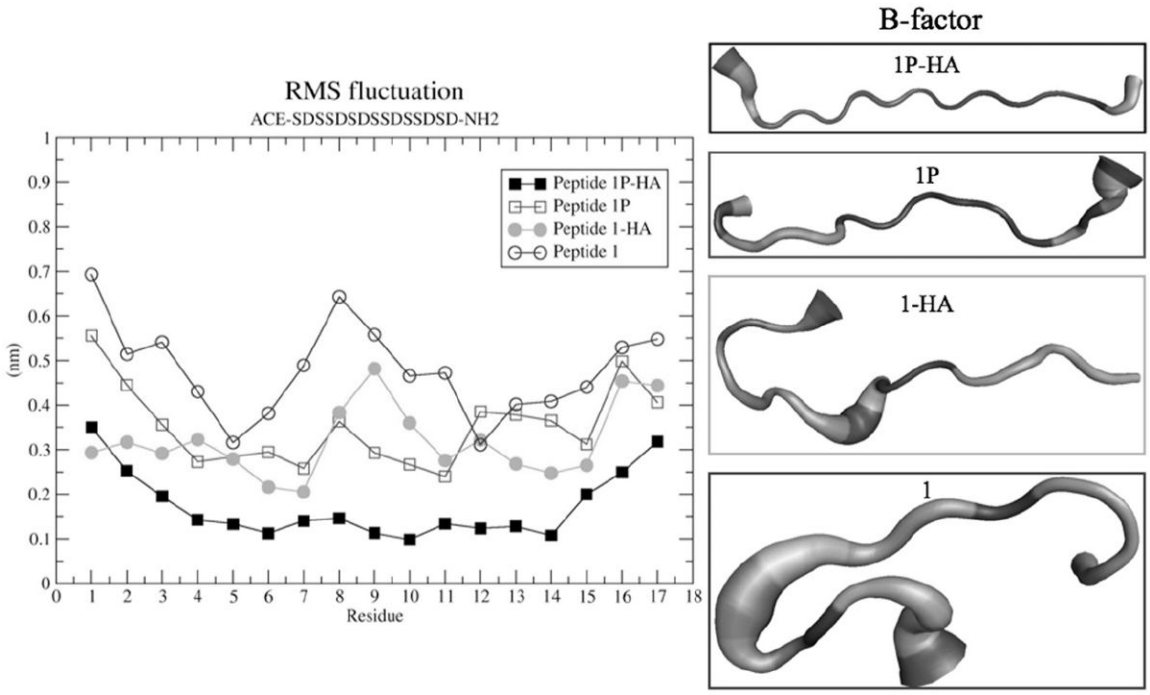

Figure 2.

Root mean square fluctuation plot (RMSF plot) calculated for all individual residues for phosphorylated peptide (peptide 1P-HA and peptide 1P) and unphosphorylated peptide (Peptide 1 and Peptide 1-HA). The B-factor analysis showed the average structures.

Table 1

Peptides investigated.

Peptide number	Sequence	Total charge (q)
Peptide 1	Ace-SDSSDSDSSDSSDSD-NH2	−6
Peptide 1P	Ace-SDSpSDpSDpSpSDpSpSDpSD-NH2	−20
Peptide 2	Ace-SSDSKSDSSKSESDS-NH2	−4
Peptide 2P	Ace-SSDpSKpSDpSpSKpSEpSDS-NH2	−16
Peptide 3	Ace-SSDSSDSSSSSDSSN-NH2	−3
Peptide 3P	Ace-SSDSpSDpSpSpSSpSDSSN-NH2	−13
Peptide 4	Ace-SSNSSDSSNSSDSSN-NH2	−2
Peptide 4P	Ace-SSNSSDpSSNSpSDSSN-NH2	−6
Peptide 5	Ace-SSDSSDSSDSSDSSD-NH2	−5
Peptide 5P	Ace-SSDpSpSDpSpSDpSpSDpSpSD-NH2	−22

The peptides used in this study were taken from the conserved sequence of the DPP and they were phosphorylated according NetPhos 2.0 server.